J Mater Sci (2014) 49:4270–4278
DOI 10.1007/s10853-014-8122-6

New insight into PEO modified inner surface of HNTs and its nano-confinement within nanotube

Shuyan Yang · Zhimeng Liu · Yuanqi Jiao · Yuping Liu · Chuanwei Ji · Yanfang Zhang

Received: 7 January 2014 / Accepted: 20 February 2014 / Published online: 6 March 2014

Abstract In this study, we demonstrate the use of poly (ethylene oxide) (PEO) for in-situ modification of the inner surface of halloysite nanotubes (HNTs) with water molecules as the hydrogen bond forming medium, as well as the nano-confinement of PEO molecular chains within the nanotube. Before testing, the Soxhlet experiment of PEO/HNTs powder is applied in order to remove the physical adsorption of PEO molecules onto the outmost surface of HNTs. The crystal temperature of PEO changes sharply from 36.9 °C of neat PEO to −25 °C of PEO in the PEO/HNTs powder and the decomposed temperature of PEO in the PEO/HNTs powder is about 13.1 °C higher than that of neat PEO, which is mainly owing to the nano-confinement effect of PEO within the HNTs with a diameter of about 10 nm. From thermo-gravimetric (TG) analysis, about 7.71 % by weight of PEO has been chemically bonded to HNTs. The hydrogen bonds among PEO, HNTs, and water molecules are evidenced by FTIR and XPS performances. Meanwhile, the binding energy of Al_{2p} in the innermost surface of HNTs shifts from 74.7 eV in the neat HNTs to 74.5 eV in the PEO/HNTs powder, while that of Si_{2p} on the outmost surface of HNTs keeps almost constant, indicating that the hydrogen bonds only exists inner the nanotube and PEO molecular chains have been trapped in nano-scale within HNTs, which is in accordance with the DSC and TG observation.

S. Yang · Z. Liu (✉) · Y. Jiao · Y. Liu · C. Ji · Y. Zhang
Chemical Industrial Cleaner Production and Green Chemical R&D Center of Guang Dong Universities, Dongguan University of Technology, Dongguan City 523808, People's Republic of China
e-mail: zmliu1234@126.com

S. Yang · Z. Liu · Y. Jiao · Y. Liu · C. Ji · Y. Zhang
Dongguan Cleaner Production Center, Dongguan City 523808, People's Republic of China

Introduction

In recent years, polymer nanocomposites, especially including inorganic filler with at least one-dimension in nano-scale, have attracted considerable interest [1, 2], both in academia and in applied polymer industry, due mainly to their excellent performances such as high mechanical properties [3], thermal stability [4, 5], gas permeation resistance [6], fire retardant [7], and physical properties [8]. Two major reasons may be responsible for properties improvement in polymer nanocomposites. One is the well-dispersion degree of inorganic filler in the polymer matrix because particle aggregation, caused by thermodynamic driving force, will introduce more defects in the nanocomposites, leading to a catastrophic effect for nanocomposites. Another is the interaction between polymer matrix and inorganic filler as strong interaction will allow stress to pass from polymer chains to inorganic filler in the form of chain relaxation when an external stress is applied to the nanocomposites [9]. For these purposes, many efforts of filler modification, such as silane coupling agent modification [8], in-situ carboxyl [1] or its salts [9] modification, ionic liquid modification [10], surface-initiated atom transfer radical polymerization (SI-ATRP) modification [11], etc., have been made in order to acquire good comprehensive performances of nanocomposites.

In all the inorganic fillers, halloysite nanotubes (HNTs) are a unique and facile nature mineral, with silica on the outermost surface and alumina (Al–OH) in the innermost surface [12, 13], as shown in Scheme 1. Kaolinite plates roll along the major crystallographic directions to form

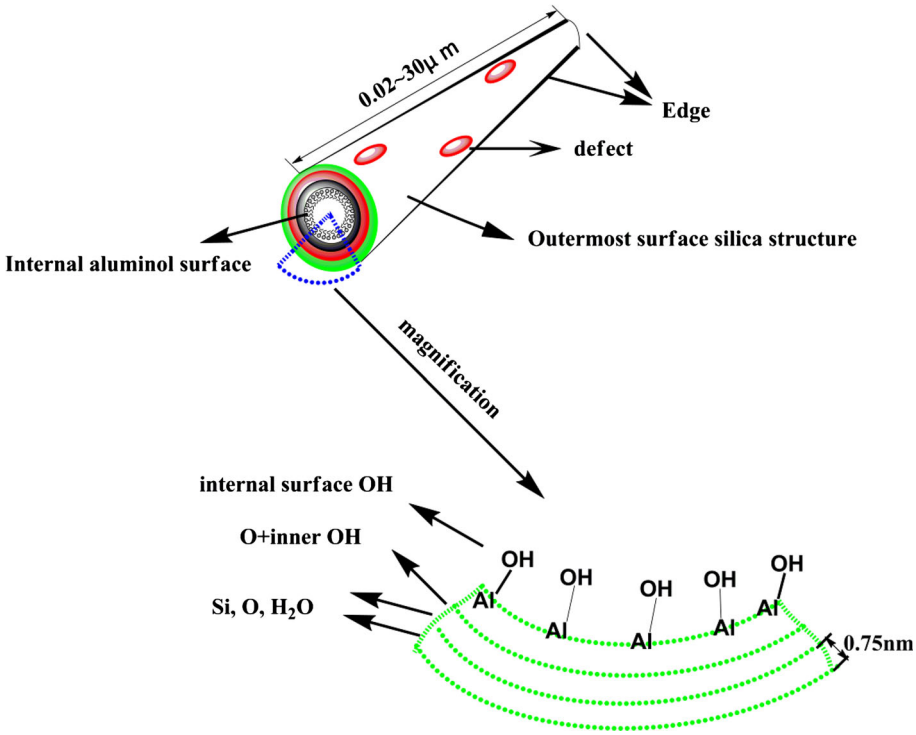

Scheme 1 Typical diagrams for the structure of a halloysite nanotube

tubes identical to proper tubular halloysite under hydration [12], providing a curling structure. Moreover, defects on the surface of halloysite, such as surface breakage, probably results from mechanical damage or crystallographic defects [14] (Scheme 1). Recently, it has reported that HNTs have typical dimensions of 10–50 nm in outer diameter, 5–20 nm in inner diameter with the lengths in a wide range from 0.02 to >30 μm [15, 16], typical specific surface area of 65 m^2/g and pore volume of ~1.25 mL/g. These unique structure characteristics, such as high surface area, large aspect ratio and hollow structure, make HNTs a promising candidate for low-density nanocomposites, taking the place of larger quantities, as well as high price, of macro- or micro-counterparts such as glass or carbon fibers. Modification of edges/defects of the halloysite tube outer surface is intended to be a particularly versatile approach to surface modification, with the purpose of improving clay dispersion in polymer matrix or fluidic material [9, 10, 17–19]. However, reports on the modification of the innermost surface hydroxyl group of HNTs are rarely delivered [11]. Peng et al. [14] found that the direct grafting of γ-aminopropyl-triethoxysilane (APTES) onto the hydroxyl groups of the internal walls, edges and external surfaces of HNTs is valid, based on the consideration of the thermal and evacuation pretreatment conditions by controlling the extent and mechanism of the modification. Another interesting finding is that the extent of modification is also strongly affected by the morphological parameters of the original clay samples. Weng et al. [11, 20] believed that selective interior modification by immobilization of functional groups via covalent bonds could open up new applications based upon molecular recognition. In their works [11], the use of a catecholic anchor (Dopa) for selective modification of the inner surface of HNTs has been reported, following by SI-ATRP through selectively adsorbing Dopa to graft a layer of polymer brush into the nanotube lumen. In the polymer/inorganic filler nanocomposites, the modification of inorganic filler through water as a hydrogen bond forming medium, to our knowledge, has not yet been explored.

In this study, a novel approach is introduced to modify HNTs with water naturally existed in the lumen of HNTs as a hydrogen bond forming medium between HNTs and poly (ethylene oxide) (PEO) by solution mixing method. The PEO/HNTs nanocomposite is extracted by methyl cyanide with a Soxhlet extractor for 24 h, sequentially following by Fourier transform infrared spectroscopy (FTIR) and X-ray photoelectron spectroscopy (XPS) measurement to evaluate the hydrogen bonding interactions among PEO, HNTs, and water molecules. Furthermore, thermo-gravimetric analysis (TGA) and differential scanning calorimetry (DSC) are performed to confirm the interaction incident and nano-confinement of PEO occurred within the lumen of HNTs.

Experimental section

Materials

PEO, the number average molecular weight of 2.0×10^5, from Sigma-Aldrich was used as one of the mixing components. HNTs, was mined from Hubei, China and further treated according to the procedure [21] and dried in an vacuum oven at 80 °C for 12 h. Methyl cyanide was analytical reagent grade.

Preparation of PEO/HNTs powder

About 0.2 g HNTs was first dispersed in 10 mL methyl cyanide within a single neck flash for 10 min under room temperature. After that, the mixing solution was ultrasonically treated for 30 min, following by a vigorously stir. Then about 0.5 g PEO was added, the vigorously stir continued for another 3 h. The PEO/HNTs film was achieved by pouring the mixing into a home-made model and evaporating the solvent in a fume hood at room temperature for 12 h.

Soxhlet extracting experiment was carried out in order to remove the PEO molecular chain adsorbed to the surface of HNTs by physical adsorbing effect. Sufficient dosage of methyl cyanide was poured into a single neck flask equipped with Soxhlet extractor and condenser pipe in the purpose of refreshing the good solvent for PEO. Then, the PEO/HNTs film sealed by 400 mesh filtration fabric and filter paper was placed in the Soxhlet extractor, following by a heating incident of 95 °C for 24 h. After that, the PEO/HNTs powder was dried in a vacuum oven at 60 °C until the powder weight kept constant.

Characterization

DSC analysis

The crystalline behavior of PEO in the PEO/HNTs powder was examined using a Netzsch DSC 200F3 Instrument. Before testing, the PEO/HNTs powder was kept at a constant temperature of 60 °C for 12 h. Sample of approximately 10 mg was sealed in aluminum pans and performances were carried out with a heating rate of 10 °C/min, in the temperature range 20–110 °C, under a nitrogen atmosphere. The sample was held at 110 °C for 10 min, following by a heating incident from 110 to −40 °C with a heating rate of −10 °C/min.

TG analysis

The thermal decomposition behaviors of HNTs, PEO, and PEO/HNTs powder were determined using a thermogravimetric analyzer (TG-209F3, the Netzsch Company) in the temperature range of 25–650 °C with a scanning rate of 10 °C/min under nitrogen atmosphere.

FTIR analysis

The FTIR analysis was conducted by a Bruker Tensor 27 spectrometer at room temperature. Spectra were taken from 400 to 4000 cm^{-1} with resolving power of 4 cm^{-1}.

XPS analysis

It had been reported that the wall thickness of HNTs was about 20 nm [20], which exceeded the penetration depth of XPS (about 10 nm). However, since defects on the surface of HNTs, such as surface breakage, and HNTs oriented on the substrate randomly occurred, the chemical bonding in the inner surface may be partially exposed to X-ray [20]. Thus, XPS would be competent for examination of chemical bonding within the lumen of HNTs. XPS spectra of HNTs, PEO, and PEO/HNTs powder were recorded by using an X-ray photoelectron spectrometer (LVAC-PHI 1800, Ulvac-Phi Company) with an aluminum (mono) K_a source (1486.6 eV). The aluminum K_a source was operated at 15 kV and 10 mA. All core level spectra were referenced to the C_{1s} neutral carbon peak at 284.7 eV.

Results and discussion

Evidence for nano-confinement of PEO within HNTs

It is well known that the effect of interactions [22, 23], as well as the confinement in the hollow [24, 25] or cross-linking structure [26], between two mixing compounds will be of significant importance on the crystalline temperature of crystalline compounds. In our previous work [22], we found that the weak intermolecular interaction between NBR and PEO would cause a dramatic decrease in the crystal melting temperature of PEO, from 69.9 °C of neat PEO to 59.5 °C of PEO/NBR blended with the ratio of 5:95, which is also valid for strong molecular interaction reported by Yen et al. [23]. When the confinement of PEO reduces to nano-scale, an interesting phenomenon that the crystal melting temperature and crystal temperature of PEO decrease to sufficiently low can be obtained [24, 25], which also calls crystal melting temperature depression and crystal temperature depression, respectively. As described in Ref. [23–25], only the nano-confinement of PEO molecular chains can lead to a great decrease, below zero, in the crystal temperature of PEO, which is a valid approach to probe the nano-confinement of crystal polymers within nanotubes [25].

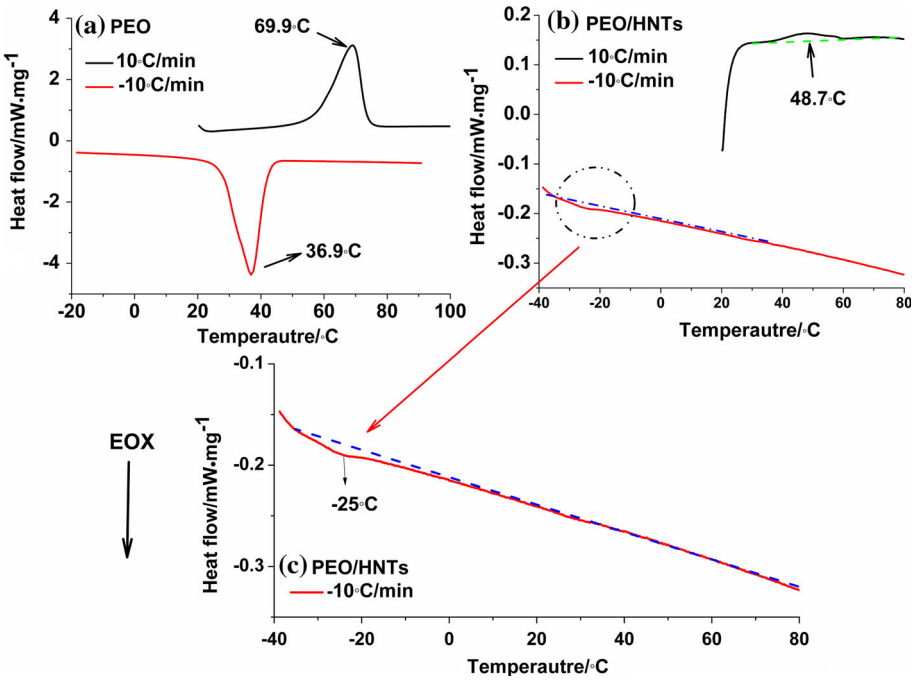

Fig. 1 Crystal melting temperature and crystal temperature of PEO: **a** neat PEO; **b**, **c** PEO/HNTs powder

In Fig. 1a, the crystal temperature and crystal melting temperature of neat PEO are about 69.9 and 36.9 °C, respectively. For accurate illumination of nano-confinement of PEO in HNTs, in this study, PEO/HNTs powder was pretreated by Soxhlet extracting experiment in order to remove the PEO molecular chains physically adsorbed to the surface of HNTs. In Fig. 1b, the crystal melting temperature of PEO in the PEO/HNTs powder is about 48.7 °C, about 21.2 °C lower than that of neat PEO [22]. We speculate that the crystal melting temperature depression may be due to the decrease in PEO crystallite size (nano-confinement) and the increase in the interfacial area [25, 27]. If PEO molecular chains chemically bonded to the surface of HNTs that cannot be eliminated by Soxhlet extracting experiment, the crystal temperature of PEO would lie above zero, neighboring the crystal temperature of neat PEO [23]. The crystal curve of PEO in the PEO/HNTs powder is also shown in Fig. 1b, it is clear that when the temperature is above zero, not any exothermal peak can be found, indicating that there is not any PEO molecular chains on the surface of HNTs. Meanwhile, a much greater crystal temperature depression, from 36.9 °C of neat PEO to −25 °C of PEO in the PEO/HNTs powder, of about 61.9 °C is acquired, as shows in Fig. 1c. Yu et al. [24] suggested that when PEO molecules was trapped in nano-scale confined spaces, for instance 100 nm confined space, the crystal temperature of PEO reached −18.6 °C. With decreasing pore diameter, the crystal temperature decreased subsequently. As the pore diameter decreased to 10 nm, the crystal temperature could get to as far as −25.1 °C. The dimension of PEO monoclinic unit cells is about 1 nm [28], in our laboratory [29] and other studies [15, 16], the inner diameter of HNTs is about 10 nm. In Fig. 1c, the crystal temperature of PEO in the PEO/HNTs powder is about −25 °C, suggesting that PEO molecular chains have be trapped within HNTs.

TGA analysis

For organic modified inorganic filler, it is universally known that two thermo-gravimetric (TG) platforms, representing the thermal decomposition of organic component at low temperature and thermal behavior of inorganic part at higher temperature, can be found in the TG curves [30]. In Fig. 2, only one decomposed platform is observed in the TG traces of HNTs and PEO, with the decomposed temperature for HNTs and PEO at 443.2 and 331.7 °C, respectively. However, the thermal curve of PEO/HNTs powder shows two decomposed platforms when compared to PEO or HNTs. The first decay is attributed to the loss of PEO with the decomposed temperature of 344.8 °C, which is 13.1 °C higher than that of neat PEO owing to the nano-confinement of PEO within HNTs. This is in accordance with the result of the PEO nano-confinement from the DSC measurement of PEO/HNTs powder in "Evidence for nano-confinement of PEO within HNTs" section. Another one locates at the decomposed temperature of 446.5 °C, assigning to the dehydroxylation step of HNTs. Moreover, calculated from the TG trace of PEO/HNTs powder, one can get that about 7.71 % by weight of PEO has been chemically bonded to HNTs, which cannot be removed by

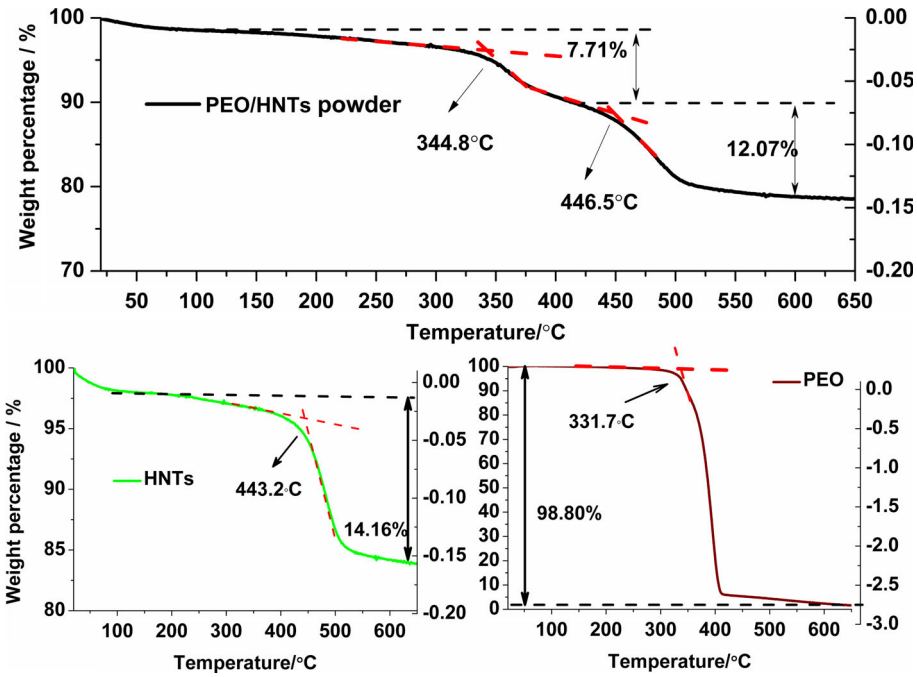

Fig. 2 The thermo-gravimetric traces and their first derivative curves of HNTs, PEO, and PEO/HNTs powder

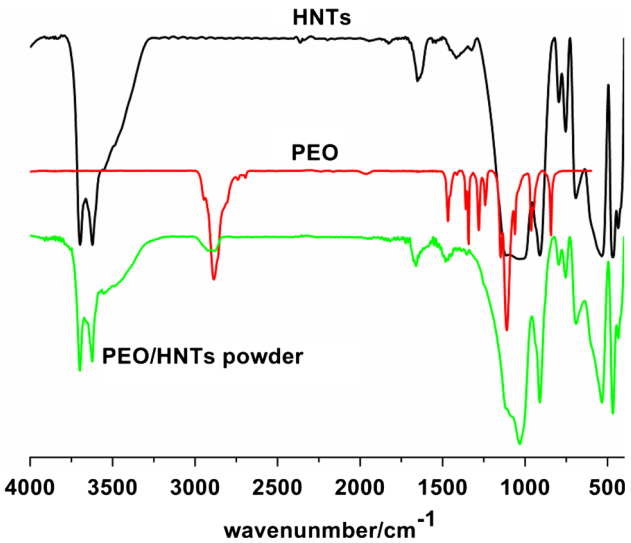

Fig. 3 The FTIR spectra of HNTs, PEO, and PEO/HNTs powder

Table 1 The characteristic wavenumbers (cm^{-1}) of HNTs, PEO, and PEO/HNTs powder

Sample	HNTs	PEO	PEO/HNTs powder
Inner surface O–H stretching	3697	–	3699
Inner O–H stretching	3622	–	3625
O–H stretching of water	3559	–	3548
$–CH_2–$	–	2886	2878
O–H deformation of water	1652	–	1677
–C–O–C–	–	1111	1106
In-plane Si–O stretching	1033	–	1033
Perpendicular Si–O stretching	692	–	691
Deformation of Al–O–Si	535	–	534
Deformation of Si–O–Si	468	–	467
Deformation of Si–O	435	–	434

the good solvent for PEO in the Soxhlet experiment, indicating that a strong interaction has formed between PEO and HNTs.

FTIR spectroscopy

FTIR spectra of HNTs, PEO, and PEO/HNTs powder in the whole region are shown in Fig. 3 and the details of the frequency and assignments of each vibrational mode observed are displayed in Table 1. The inner surface –OH and inner –OH stretching of HNTs are known to give two bands at 3697 and 3622 cm^{-1} [14, 21], while that for PEO/HNTs powder locates at 3699 and 3625 cm^{-1}, respectively, not obvious changes can be found. The broad peaks of water, –OH stretching and –OH deformation, shift from 3559 and 1652 cm^{-1} [14] in the HNTs to 3548 and 1677 cm^{-1} in the PEO/HNTs powder, separatively, indicating the chemical environment of H_2O in the PEO/HNTs powder would be different from that in the HNTs. Furthermore, a sharp peak at 2886 cm^{-1} in the PEO spectrum is attributed to the stretching of methylene ($–CH_2–$) [22]. For the PEO/HNTs powder, a red shift, about 8 cm^{-1}, can be observed, which indicates a more constricted vibration of methylene groups existed in the PEO/HNTs powder. Similar phenomenon can be found in the –C–O–C– stretching of PEO and PEO/HNTs powder. All the

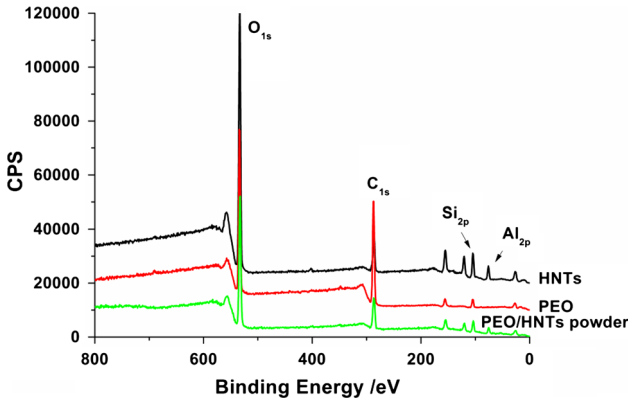

Fig. 4 XPS spectra taken for HNTs, PEO, and PEO/HNTs powder

observations mentioned above would provide us with a new understanding that a new type of chemical bond, hydrogen bond, may be formed among PEO, HNTs, and water molecules.

Moreover, compared HNTs with PEO/HNTs powder, there are not distinct difference in the in-plane Si–O stretching, perpendicular Si–O stretching, deformation of Al–O–Si, deformation of Si–O–Si and deformation of Si–O. As we mentioned above, HNTs possess a unique microstructure with silica on the outermost surface and alumina (Al–OH) in the innermost surface [12, 13], this suggests that not any interactions between PEO and outmost surface silica structure of HNTs can be found.

XPS analysis

It is well known that the formation of a new chemical bonding would lead to the variation of the chemical environment, which can be revealed by the variation of the binding energy of certain atoms via XPS survey [9]. The whole XPS spectra and fitting curves of their certain characteristic atoms of HNTs, PEO, and PEO/HNTs powder are depicted in Figs. 4 and 5 and their precise binding energies of characteristic atoms are also displayed in Table 2. As one can be seen from Table 2, the O_{1s} spectrum of HNTs is asymmetric and can be divided into two components attributed to oxide component (532.1 eV) and adsorbed water (533.0 eV) [31], whereas for PEO/HNTs powder, the O_{1s} spectrum can be analyzed in terms of three components, that is, 531.4 eV (the oxide component), 532.2 eV (PEO component), and 533.3 eV (adsorbed water), respectively. Meanwhile, the binding energy of O_{1s} in PEO locates at 532.6 eV. The great differences in the

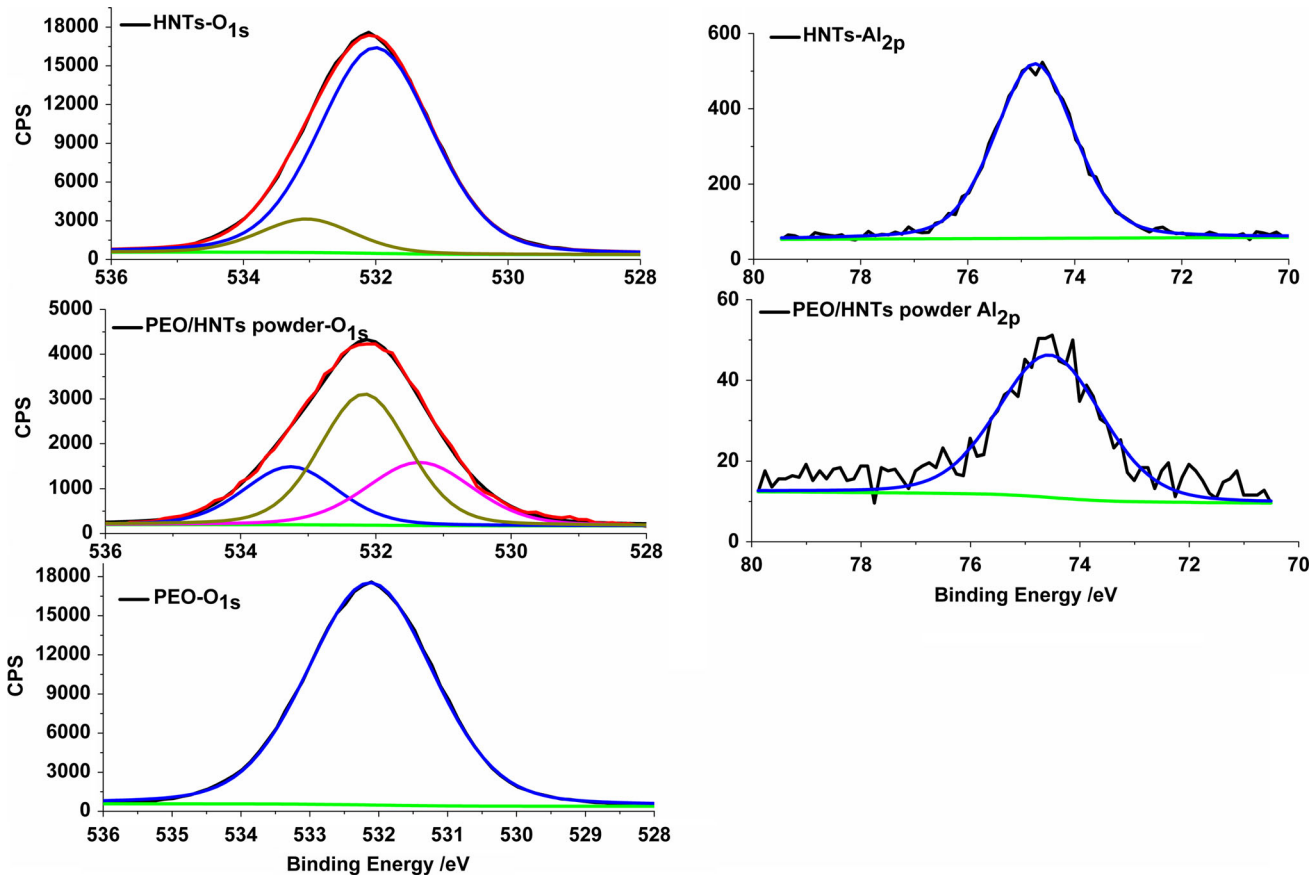

Fig. 5 Fitting curves of certain characteristic atoms of HNTs, PEO, and PEO/HNTs powder

Table 2 Binding energies of characteristic elements of HNTs, PEO, and PEO/HNTs powder

Sample	HNTs	PEO	PEO/HNTs powder
C_{1s}	–	284.6	284.6
	–	285.7	285.6
	–	286.6	286.8
	–	287.7	288.9
O_{1s}	532.0		531.4
	–	532.6	532.2
	533.0	–	533.3
Al_{2p}	74.7	–	74.5
Si_{2p}	103.1	–	103.0

binding energies of O_{1s} among HNTs, PEO, and PEO/HNTs powder suggests the hydrogen bonds have been formed among PEO, HNTs and water molecules, which also causes the binding energy of C_{1s} of PEO (286.8 eV) in the PEO/HNTs powder shifts to higher value, about 0.2 eV higher than that of PEO. Furthermore, the binding energies of Al_{2p} and Si_{2p} in HNTs are 74.7 and 103.1 eV, separately. When combining with PEO, the binding energies of Al_{2p} and Si_{2p} of HNTs are 74.5 and 103.0 eV, respectively. As mentioned above, HNTs is form by rolling Kaolinite plates along the major crystallographic directions under a certain geological condition, with silica on the outermost surface and alumina (Al–OH) in the innermost surface. The almost unchanged in the binding energy of Si_{2p} in HNTs suggests that no chemical bonding occurs between PEO and outer surface silica of HNTs, which is in accordance to the results from FTIR analysis. The binding energy of Al_{2p} in the innermost surface of HNTs shifts toward lower level, illuminating that the interaction between PEO and HNTs occurs inside the nanotube, which agrees with the results from crystal temperature depression of PEO within PEO/HNTs powder in "Evidence for nano-confinement of PEO within HNTs" section.

Combined the results from FTIR and XPS measurements, one can see that the hydrogen bond is evidently formed between PEO and HNTs inside the HNTs with water molecules as hydrogen bond forming medium.

Discussion of PEO nano-confinement within HNTs

PEO nano-confinement within HNTs can be explained in Fig. 6. When PEO is mixing with HNTs in solvent, PEO molecular chains (smaller enough than the inner pore diameter of HNTs) can migrate into the inner surface of HNTs owing to thermodynamic driving force and subsequently, interactions among PEO, HNTs and water molecules occur, as displayed in Fig. 6, leading to the diffusion limitation of PEO molecular chains, which is one of the reasons responsible to crystal temperature depression. Another reason, the most important one, is the nano-scale confinement [32, 33] of PEO. The nano-scale restriction of PEO within HNTs prohibits the configuration and reorientation of PEO molecular chains, resulting in more "freezing" effect on molecular segment motion. For PEO confined in HNTs, the melt is divided by HNTs into abundant nano-scale domains, in which a surface nucleation mechanism is more suitable for PEO crystallization

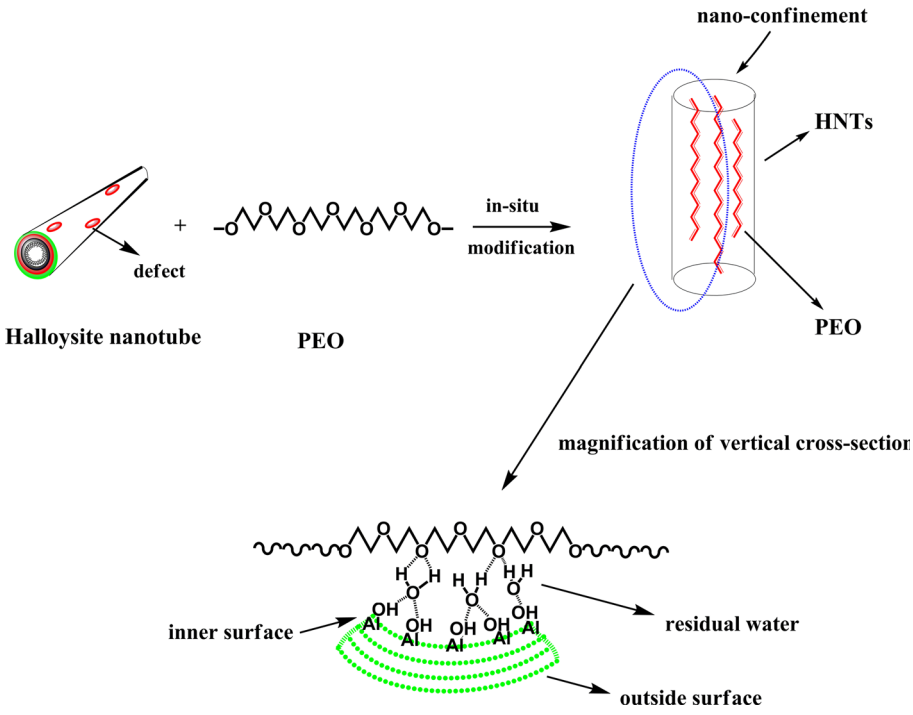

Fig. 6 The interaction among PEO, HNTs, and water in the PEO/HNTs powder

[25], as shown in Fig. 6. The surface nucleation site can only influence an "infinitesimal" fraction of molecular segment due to the interaction and nano-scale confined effect of HNTs, therefore, a larger supercooling is needed to overcome the larger free energy barrier [34], leading to a greater decrease in the crystal temperature of PEO.

Conclusions

PEO in-situ modified HNTs with water molecules as the hydrogen bond forming medium has been successfully obtained. The Soxhlet experiment of PEO/HNTs powder is applied in order to remove the physical adsorption of PEO molecules onto the outmost surface of HNTs. The crystal temperature of PEO shifts dramatically from 36.9 °C of neat PEO to −25 °C of PEO in the PEO/HNTs powder by DSC measurement, which is attributed to the nano-scale confinement effect of PEO within the HNTs with a pore diameter of about 10 nm. Calculated from the TGA trace of PEO/HNTs powder, the decomposed temperature of PEO in the PEO/HNTs powder is about 13.1 °C higher than that of neat PEO owing to the nano-confinement of PEO within HNTs. Also, one can get that about 7.71 % by weight of PEO has been chemically bonded to HNTs, which cannot be removed by the good solvent of PEO. The chemical bonds introduced to PEO/HNTs powder are explored by FTIR and XPS measurements. The wavenumber of –OH stretching of water molecules changes from 3559 cm^{-1} in HNTs to 3548 cm^{-1} in the PEO/HNTs powder. Meanwhile, the great discrepancy in the binding energies of O_{1s} in HNTs, PEO, and PEO/HNTs powder can be observed, illuminating that hydrogen bond has been formed among PEO, HNTs, and water molecules. Furthermore, the binding energy of Al_{2p} in the innermost surface of HNTs in the PEO/HNTs powder shifts toward lower level, while that of Si_{2p} on the outmost surface of HNTs and PEO/HNTs powder keeps almost constant, indicating the interaction between PEO and HNTs occurs inside the nanotube, which is also confirmed by the result from FTIR analysis that not any difference of in-plane Si–O stretching on the outmost surface of HNTs and PEO/HNTs powder is detected. All the experimental data support a fact that hydrogen bonds have been introduced between PEO and HNTs by water molecules as modified medium in the inner surface of HNTs and PEO molecular chains have been trapped in the nano lumen of HNTs.

Acknowledgements The authors gratefully acknowledge the financial support from The National Natural Science Funds of China (No. 51303026), Science Foundation for Universities and Institutions of Dongguan City, P. R. China (Grant No. 2012108102008) and the Research Fund for the Doctoral Program of Dongguan University of Technology, P. R. China (Grant No. ZJ121002).

References

1. Guo B, Chen F, Lei Y et al (2009) Styrene-butadiene rubber/halloysite nanotubes nanocomposites modified by sorbic acid. Appl Surf Sci 255:7329–7336
2. Yang S, Liu L, Jia Z et al (2011) Study on the curing properties of SBR/La-GDTC/SiO_2 composites. J Rare Earths 29:444–453
3. Yang S, Liu L, Jia Z et al (2011) Study on the influence of lanthanide glutamic dithiocarbamate on the interfacial reinforcement of SBR/SiO_2 composites by swelling equilibrium test. Acta Polym Sin 52:709–719
4. Liu X, Zhao SH (2008) Measurement of the condensation temperature of nanosilica powder organically modified by a silane coupling agent and its effect evaluation. J Appl Polym Sci 108:3038–3045
5. Dohi H, Horiuchi S (2007) Locating a silane coupling agent in silica-filled rubber composites by EFTEM. Langmuir 23:12344–12349
6. Yoshinaga K, Tani Y, Tanaka Y (2002) Surface modification of fine colloidal silica with copolymer silane-coupling agents composed of maleic anhydride. Colloid Polym Sci 280:85–89
7. Guo YB, Wang LS, Zhang AQ (2006) Mechanical properties and crosslink density of rare earth-modified high-abrasion furnace-filled powdered natural rubber. J Appl Polym Sci 102:1755–1762
8. Peng HL, Liu L, Luo YF et al (2009) Effect of 3-propionylthio-1-propyltrimethoxylsilane on structure mechanical, and dynamic mechanical properties of NR/silica composites. Polym Compos 30:955–961
9. Yang S, Liu L, Jia Z et al (2011) Structure and mechanical properties of rare-earth complex La-GDTC modified silica/SBR composites. Polymer 52:2701–2710
10. Lei Y, Tang Z, Zhu L et al (2011) Functional thiol ionic liquids as novel interfacial modifiers in SBR/HNTs composites. Polymer 52:1337–1344
11. Yah WO, Xu H, Soejim H et al (2012) Biomimetic dopamine derivative for selective polymer modification of halloysite nanotube lumen. J Am Chem Soc 134:12134–12137
12. Singh B, Mackinnon IDR (1996) Experimental transformation of kaolinite to halloysite. Clay Clay Miner 44:825–834
13. Singh B (1996) Why does halloysite roll? A new model. Clay Clay Miner 44:191–196
14. Yuan P, Southon PD, Liu Z et al (2008) Functionalization of halloysite clay nanotubes by grafting with γ-aminopropyltriethoxysilane. J Phys Chem C 112:15742–15751
15. Rawtani D, Agrawal YK (2012) Multifarious applications of halloysite nanotubes: a review. Rev Adv Mater Sci 30:282–295
16. Joussein E, Petit S, Churchman J et al (2005) Halloysite clay minerals—a review. Clay Miner 40:383–426
17. Ma W, Yah WO, Otsuka H et al (2012) Surface functionalization of aluminosilicate nanotubes with organic molecules. Beilstein J Nanotechnol 3:82–100
18. Matsuno R, Otsuka H, Takahara A (2006) Polystyrene-grafted titanium oxide nanoparticles prepared through surface-initiated nitroxide-mediated radical polymerization and their application to polymer hybrid thin films. Soft Matter 2:415–421
19. Du M, Guo B, Jia D (2010) Newly emerging applications of halloysite nanotubes: a review. Polym Int 59:574–582
20. Yah WO, Takahara A, Lvov YM (2011) Selective modification of halloysite lumen with octadecylphosphonic acid: new inorganic tubular micelle. J Am Chem Soc 134:1853–1859
21. Liu M, Guo B, Du M et al (2007) Properties of halloysite nanotube–epoxy resin hybrids and the interfacial reactions in the systems. Nanotechnology 18:455703
22. Yang S, Liu Z, Jia Y et al (2013) Study on the compatibility and crystalline morphology of NBR/PEO binary blends. J Mater Sci 48:6811–6817. doi:10.1007/s10853-013-7486-3

23. Yen KC, Woo EM (2009) Formation of dendrite crystals in poly(ethylene oxide) interacting with bioresourceful tannin. Polym Bull 62:225–235
24. Guan Y, Liu G, Ga P et al (2013) Manipulating crystal orientation of poly(ethylene oxide) by nanopores. ACS Macro Lett 2: 181–184
25. Maiz J, Martin J, Mijangos C (2012) Confinement effects on the crystallization of poly (ethylene oxide) nanotubes. Langmuir 28:12296–12303
26. Lopez-Manchado MA, Valentin JL, Herrer B et al (2004) Novel approach of evaluating polymer nanocomposite structure by measurements of the freezing-point depression. Macromol Rapid Comm 25:1309–1313
27. Michell RM, Lorenzo AT, Müller AJ et al (2012) The crystallization of confined polymers and block copolymers infiltrated within alumina nanotube templates. Macromolecules 45:1517–1528
28. Ching IH, Jun-Rong C (2001) Crystallization and chain conformation of semicrystalline and amorphous polymer blends studied by wide-angle and small-angle scattering. J Polym Sci B 39:2705–2715
29. Liu M, Guo B, Du M et al (2009) Halloysite nanotubes as a novel β-nucleating agent for isotactic polypropylene. Polymer 50:3022–3030
30. Kow KW, Abdullah EC, Aziz AR (2009) Effects of ultrasound in coating nano-precipitated $CaCO_3$ with stearic acid. Asia Pac J Chem Eng 4:807–813
31. Sanjines R, Tang H, Berge H et al (1994) Electronic structure of anatase TiO_2 oxide. J Appl Phys 75:2945–2951
32. Nojima S, Ohguma Y, Namiki S et al (2008) Crystallization of homopolymers confined in spherical or cylindrical nanodomains. Macromolecules 41:1915–1918
33. Wu H, Wang W, Huang Y et al (2008) Polymorphic behavior of syndiotactic polystyrene crystallized in cylindrical nanopores. Macromolecules 41:7755–7758
34. Loo Y-L, Register RA, Rya AJ et al (2001) Polymer crystallization confined in one, two, or three dimensions. Macromolecules 34:8968–8977